RSC Sustainability

ROYAL SOCIETY OF CHEMISTRY

PAPER

View Article Online
View Journal | View Issue

Cite this: *RSC Sustainability*, 2024, **2**, 2348

Lignin-based sustainable antifungal gel nanocoatings for disinfecting biomedical devices†

Sanjam Chandna,‡[ab] Kunal Gogde,[ac] Shatabdi Paul§[ad] and Jayeeta Bhaumik *[a]

Received 17th April 2024
Accepted 19th June 2024

DOI: 10.1039/d4su00180j

rsc.li/rscsus

There is growing awareness that utilizing lignin as a sustainable biopolymer has emerged as a promising avenue to address challenges in antimicrobial protection. However, the application of lignin to prevent the spread of fungal infections is a less explored area and needs attention. Traditional antifungal agents often highlight significant concerns related to toxicity and environmental impact. To overcome these limitations, lignin, a renewable and biodegradable polyphenolic compound derived from plant cell walls, proves to be a substantial candidate. In this work, lignin is employed as a precursor molecule for the development of a gel-based coating. Rapid gelation technology was immensely useful in fabricating these versatile antifungal coatings. The developed coatings were highly transparent (nearly 85% transmittance values) and water resistant. Furthermore, the incorporation of lignin-based photodynamic nanoconjugates into coatings provides a multifaceted approach to combat fungal growth, thereby enhancing durability and sustainability, which enhanced the photodynamic activity of the lignin nanocoatings by approximately 50 fold. This work highlights the synergistic potential of lignin-based sustainable nanocoatings combined with photodynamic activity for on-demand disinfection of biomedical instruments.

Sustainability spotlight

In this work, lignin is used as a sustainable biopolymer to develop gel-based coatings through one-step and non-toxic procedures. Such a natural biomaterial-based disinfecting product developed in this work possesses properties of an adhesive coating having enhanced water resistance, which was applied through spread coating, spray coating, and dip coating techniques on biomedical devices. Lignin-based photodynamic nanoconjugates were incorporated into the developed coatings, for stimuli-responsive and controlled on-demand delivery to disinfect a wide range of biomedical devices. This scalable sustainable coating can also be applied to a broad range of fields including food preservation and agricultural applications.

Introduction

Photodynamic surface-coating materials technologies have been utilized as an innovative approach for commercial disinfection.[1] In the relentless pursuit of innovative strategies to combat microbial threats, the utilization of sustainable resources has emerged as a convincing approach for exploration. Lignocellulosic biomass, a renewable feedstock abundantly available from plant materials, has garnered significant attention for its multifaceted applications.[2] Owing to its polyphenolic structure, lignin (a complex and heterogeneous aromatic polymer) stands out as an intriguing candidate due to its unique structural attributes and inherent antimicrobial potential.[3] In recent years, there has been a growing realization of the capacity of lignin to serve as a foundation for developing novel antimicrobial coatings.[1–4] Lignin serves as a crucial determinant of structural integrity and defense against microbial invasion.[3–8] Its intricate chemical structure, characterized by an array of phenolic hydroxyl groups and aromatic moieties, suggests inherent antimicrobial activity.[8,9] Recent research has unveiled a captivating dimension of lignin's antimicrobial and anticancer potential through its photodynamic activity.[2,10] This intriguing property capitalizes on the generation of reactive oxygen species (ROS) upon light activation, leading to localized oxidative stress and subsequent microbial cell damage.[11] The aromatic chromophores present in the structure of lignin are

[a]*Center of Innovative and Applied Bioprocessing (CIAB), Department of Biotechnology (DBT), Government of India, Sector 81 (Knowledge City), S. A. S. Nagar 140306, Punjab, India. E-mail: jbhaumi@gmail.com; jayeeta@ciab.res.in*

[b]*Department of Microbial Biotechnology, Panjab University, South Campus, Sector 25, Chandigarh 160036, India*

[c]*University Institute of Pharmaceutical Sciences, Panjab University, Sector 14, Chandigarh 160014, India*

[d]*Regional Centre for Biotechnology, Faridabad 121001, Haryana, India*

† Electronic supplementary information (ESI) available: Instruments and methods, materials and chemicals, and tables. See DOI: https://doi.org/10.1039/d4su00180j

‡ Present address: Institute of Chemistry and Biochemistry, Freie Universität Berlin, 14195 Berlin, Germany.

§ Present address: Department of Pharmaceutical Technology (Process Chemistry), National Institute of Pharmaceutical Education and Research, S. A. S. Nagar, 160062, Punjab, India.

capable of absorbing light within a specific wavelength range and play a pivotal role in initiating this photochemical cascade.[12] By harnessing lignin's inherent ability to generate ROS under controlled light conditions, there lies an immense opportunity to explore the prospects of developing photodynamic antimicrobial coatings.[12] For instance, the preparation of an efficient antiviral coating has recently been published by a group of researchers using spin coating technology.[1] The antiviral mechanism was attributed to the ROS production from lignin on exposure to visible light. Also, the coating was stable under ambient conditions for up to six months.[13] Other important advantages of utilizing lignin include: biodegradability, sustainability, cost-effectiveness, mechanical strength, biocompatibility and thermal stability. These attributes confer an additional advantage to lignin as compared to other synthetic polymers such as polyacrylamide and polyethylene glycol. Lignin's functional properties such as inherent antimicrobial potential, antioxidant potential and UV-protection confer an advantage over other natural polymers such as alginate, starch, and gelatin-based hydrogels.

Microbial colonization and biofilm formation pose formidable challenges across diverse sectors, ranging from healthcare and food safety to industrial processes and infrastructure.[3,4] *Candida* spp. are known to cause an increasing proportion of medical device-related infections. These organisms produce biofilms, leading to the adhesion of microorganisms to biomedical devices and other materials.[10,14,15] Conventional antifungal agents have long been employed to address these challenges. However, their widespread use has led to the emergence of resistant strains, environmental concerns, and health risks.[16,17] Antifungal coatings play a pivotal role in safeguarding various substrates, such as textiles, medical devices, and food packaging, against fungal colonization and degradation.[18] On the other side, Rose Bengal (RB) is a U.S. Food and Drugs Administration (FDA) approved photosensitizing agent known as a textile dye that can be potentially used in the biomedical field.[19] The quest for environmentally benign and effective alternatives has led researchers to explore nature-inspired solutions, and lignin has emerged as a promising contender.[20] Lignin-based silver nanoparticles have been reported to eradicate multidrug-resistant bacteria.[21] Hence, conjugation of Rose Bengal on lignin-derived silver nanoparticles could produce a sustainable, environment-friendly nanosized biomaterial for photodynamic therapy.[3] Photodynamic therapy, recognized for its precise and localized action against microorganisms, involves the activation of photosensitizers by specific wavelengths of light to induce cytotoxic effects.[4,11] In this line, the integration of photodynamic activity in lignin-based antifungal coatings holds immense potential.[13] Through careful design and formulation, these coatings can exhibit enhanced antifungal efficacy, while also offering the ability to trigger on-demand delivery of encapsulated therapeutic agents in response to specific external stimuli.

Such innovative approaches not only circumvent issues associated with conventional antimicrobial resistance but offer a pathway toward the design of photoactive lignin-based coatings with precise and localized bactericidal effects.[22] In this work, lignin is used as a precursor to develop gel-based coatings through simple and mild procedures. Such a novel resin developed in this work possesses properties of an adhesive coating material having enhanced water resistance, which was applied through spread coating, spray coating, and dip coating techniques. The structure of the coatings was characterized through various analytical techniques such as FTIR, rheology, fluorescence microscopy, and SEM analysis. The lignin-based photodynamic nanoconjugates were incorporated into the developed coatings, for stimuli-responsive and controlled on-demand delivery. This work will open up a realm of possibilities for transformative applications, spanning from wound dressings and medical devices to food preservation and environmental remediation. The integration of antimicrobial attributes and photodynamic capabilities presents a promising strategy to address challenges in antifungal protection while advancing the development of intelligent and sustainable coating technologies.

Results and discussion

Development of lignin-based gel-coating

Being a polymeric macromolecule, lignin offers the development of various materials, such as coatings and hydrogels. Various functional groups (such as phenolics, hydroxyl groups, *etc.*) present in lignin confer a structural advantage to lignin aiding in the development of different industrially relevant resources.[23] Considering all these aspects, lignin was utilized in this work, as a starting material for the development of a gel-based coating. The rapid gelation technology developed using lignin as a precursor polyphenolic material can be immensely useful in fabricating versatile antifungal coatings. Initially, lignin and polyvinyl alcohol (PVA) cross-link through hydrogen bonding between the various hydroxyl moieties. The cross linking between various PVA-lignin units and glyoxal can occur through the formation of acetal bonds by the reaction of hydroxyl groups (present in PVA as well as lignin) with the aldehyde groups of glyoxal at 60 °C. This results in the

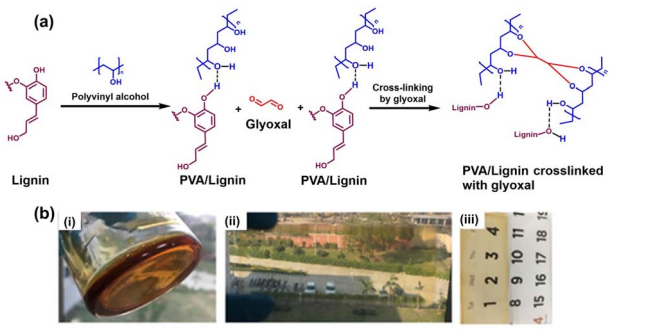

Fig. 1 (a) Prospective mechanism underlying the formation of the lignin-based gel. (b) Visual observation and transparency of the lignin-based gel (spread coated): (i) tilting of glass beaker does not lead to free flow of the gel, (ii) transparency study of the glass slide coated with lignin gel, and (iii) comparison between spread-coated (left) and uncoated (right) glass slides.

formation of intermolecular and intramolecular networks (Fig. 1a). Also, there can be a probability of forming an ester bond between PVA and lignin. Fig. 1b(i) represents the visual observation of the lignin-derived gel, and it was observed that the tilting of the glass beaker did not lead to the free flow of the developed gel. The coatings developed through lignin gel should have water-resistance properties to be industrially applicable.[24] Therefore, along with lignin, another polymer [poly(dimethyl siloxane) (PDMS)] was used as it provides industrially relevant properties to the developed lignin-based gel coatings. PDMS is a transparent elastomer, which is non-toxic and hydrophobic, can be used over a wide range of temperatures, *i.e.*, from −50 °C to 250 °C, and is relatively inert in hydrophilic solvents.[24] Rather than mixing it with the lignin gel, PDMS was coated over the glass substrates. The lignin gel was deposited over the PDMS functionalized glass substrates through three methods, namely spreading (through a fine brush), spraying, and dip coating. For spray coating, the precursor lignin gel solution was sprayed over the glass slides and then subjected to 70 °C for efficient fabrication of the developed gel onto the glass slides. However, for the spread as well as dip coating, the finally developed lignin gel was utilized. The visual observation of lignin gel-based spread coating is represented in Fig. 1b(ii). Fig. 1b(ii) and (iii) also represent the high transparency of lignin gel-based coatings through the glass material.

Characterization of the lignin-based gel-coating

After the visual observation of the developed gel, the coatings were examined under an inverted fluorescence microscope. It was observed that the developed gel coatings have a cross-linked interwoven pattern, which reveals the intense cross-linking between lignin-PVA and glyoxal. The lignin has fluorescence behavior (due to polyphenolic groups present in lignin). Therefore, the coated glass slides can be visualized *via* a fluorescence microscope. All three patterns were found to be similar as shown in Fig. 2. However, the spread-coated glass slide was found to reveal a more refined porous structure of the developed lignin gel coating. In the case of spray and dip coating, the pores were not well defined (Fig. 2). This reveals that the coating method can have a significant impact on the structure and network of the developed coating, which impacts its feasibility.

Further, the lignin-based gel coatings were characterized using transmittance studies, rheology, and Fourier transform infrared spectroscopy (FTIR) analysis. After optimization of the deposition methods of lignin-based gel coatings, the spread-coated lignin gel coatings were utilized for further analyses and application purposes. The ease of application as well as the more refined and porous structure of the spread-coated lignin gel will be helpful in the appropriate loading and release of active ingredients. The developed lignin-based gel coatings were analyzed for their surface properties, such as texture, functional groups present, and flow behavior. For this, scanning electron microscopy (SEM) was performed to visually observe the morphology of the developed coatings. It was observed that the developed coatings revealed a smooth structure. Fig. 3a depicts the SEM data obtained for the developed lignin gel coating. Further, rheology studies of the developed coatings revealed that the lignin gel coatings were viscous and stable under continuous shear and stress (Fig. 3b). Upon elemental analysis, it was found that the carbon content of the lignin gel coatings was 52%, which is similar to that of the bare lignin (57%). The results are summarized in Table S1 (ESI).† Further, the lignin gel coatings were tested for their surface functionalization through FTIR analysis. It was observed that the lignin-based gel coatings have similar functional groups to bare lignin, the functional groups majorly being polyphenolic as revealed by a major dip at 3334 cm^{-1} and a peak at ∼1050 cm^{-1} indicates the presence of C–O–C stretching vibrations of acetal bonds (Fig. 3c and d).

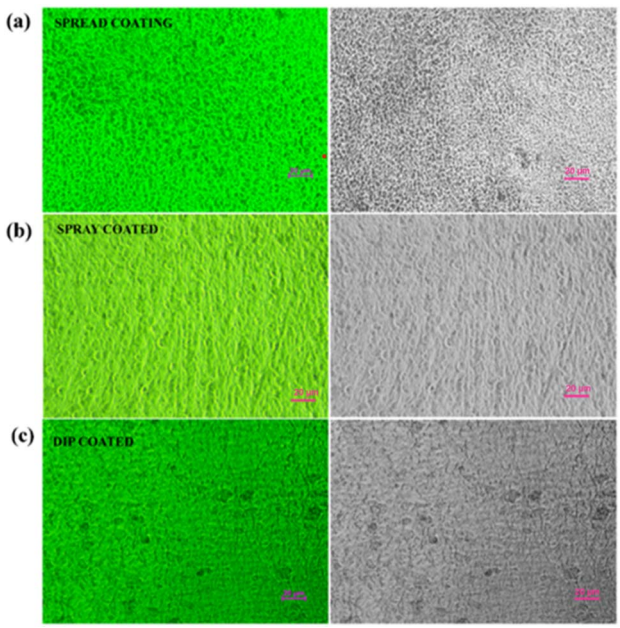

Fig. 2 Fluorescence microscopy analysis of lignin gel-based coatings (at 20 μm scale) on a PDMS functionalized glass slide: (a) spread coated, (b) spray-coated and (c) dip-coated.

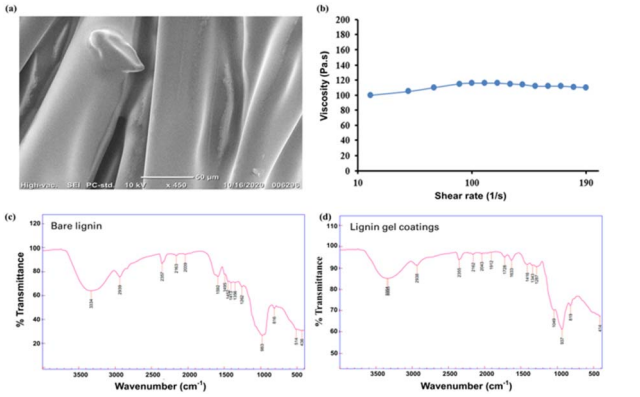

Fig. 3 (a) Scanning electron microscopy (SEM) of lignin-based gel coating, (b) rheology studies, (c) FTIR analysis of bare lignin, and (d) FTIR analysis of lignin gel coatings.

Development and characterization of RB@AgLNCs doped lignin gel nanocoatings

After the thorough and detailed characterization of the developed lignin-based gel coatings, the lignin gel was doped with lignin-based silver nanoparticles (AgLNCs) conjugated with Rose Bengal (RB@AgLNCs). The synthesis of RB@AgLNCs is adapted from our previous work.[3] For this, the bioinspired RB@AgLNCs (5% w/v) were mixed with the lignin gel precursor solution and left for half an hour under stirring at 70 °C. This has led to proper homogenization as well as the incorporation of nanoconjugates into the developed lignin-based gel for antimicrobial photodynamic therapy applications.

To confirm the incorporation of RB@AgLNCs into the lignin gel coatings, the lignin-based bare gels as well as the newly developed lignin gel-based nanocoatings were analyzed using UV-Vis spectroscopy (Fig. 4a). It was observed that there was a single major peak corresponding to lignin present in the bare lignin gel. However, the lignin gel-based nanocoating (comprising RB@AgLNCs) revealed the peak of lignin (280 nm) along two other peaks for RB@AgLNCs (560 nm for RB and 420 nm for AgLNCs). Moreover, the AgLNCs doped lignin gel coating was also analyzed as a control, which revealed two peaks for lignin (280 nm) and AgLNCs (420 nm). This study confirms the presence of nanoconjugates inside the lignin-based gel.

Since Rose Bengal is a fluorescent dye, the incorporation of such a dye into the lignin gel coating significantly increases the fluorescent properties of the finally developed lignin gel nanocoatings. Therefore, the probes were tested for their fluorescence spectra, which revealed that the bare lignin gel coating was also fluorescent to some extent (Fig. 4b). However, the Rose Bengal doped lignin gel coatings were found to be highly fluorescent, and lignin-based silver nanocomplexes also added to the fluorescence properties (Fig. 4c and d). Upon careful evaluation of the fluorescence spectra (Fig. 4b–d), it was observed that the peak for the fluorescence spectra of bare lignin coatings is centered at ~500 nm (Fig. 4b), which shows a significant shift towards ~590 nm. This can be attributed to the interaction between lignin and Rose Bengal, causing possible changes in the local environment and interactions.

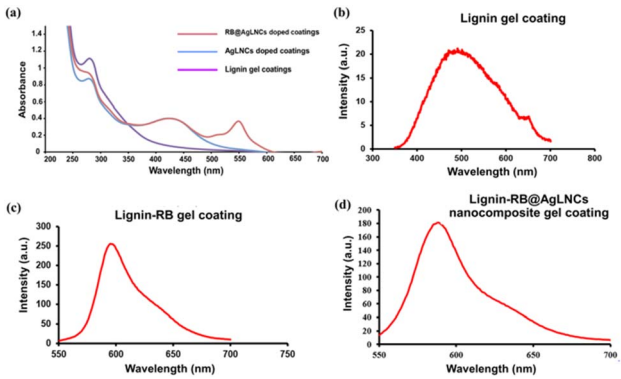

Fig. 4 Spectroscopic analysis: (a) UV-vis spectra of the RB@AgLNCs doped lignin gel coating, AgLNCs doped lignin gel coatings and bare lignin gel coatings, (b) fluorescence spectrum of lignin gel (λ_{ex} = 365 nm), (c) fluorescence spectrum of the lignin-RB gel coating (λ_{ex} = 525 nm), and (d) fluorescence spectrum of the lignin-RB@AgLNCs gel coating (λ_{ex} = 525 nm).

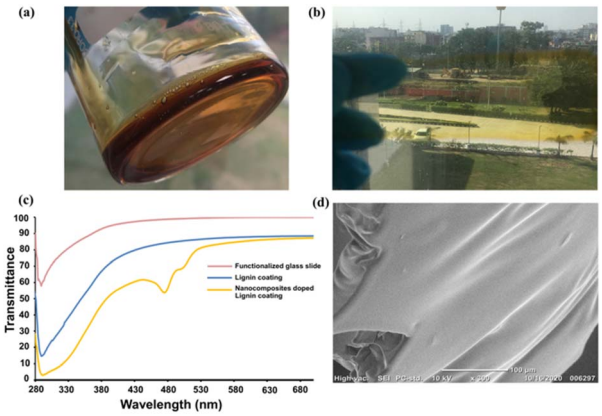

Fig. 5 Visual observation and morphological analysis of the developed lignin-based nanocomposite gel: (a) visual observation of free-flowing analysis of the developed gel; (b) transparency analysis of lignin nanocomposite gel-based coating. (c) Transmittance analysis of the bare lignin gel coating; (d) SEM analysis of the lignin nanocomposite gel-based coating.

These interactions could induce electronic coupling between their energy levels, which can change the energy levels available for electronic transitions and fluorescence emission, leading to a shift in the emission wavelength. The specific molecular arrangement and orientation of lignin and Rose Bengal within the coating can play a significant role in this phenomenon. It was speculated that the lignin nanogel was consistent with the bare lignin gel and resisted the free flow as well (Fig. 5a). When tested for transparency properties, the lignin-based nanocoatings had a color tint due to the presence of silver-based nanoconjugates. However, the transparency of the lignin-gel-based nanocoatings was consistent and maintained (Fig. 5b).

For efficient antimicrobial photodynamic therapy, the developed coatings need to be transparent, so that the light can penetrate to a maximum extent inside the developed coatings.[25] Therefore, the PDMS functionalized glass slide, lignin gel-coated glass slide and glass slide coated with lignin gel nanocoatings were evaluated for their transmittance properties using a UV-vis spectrophotometer. It was found that the PDMS functionalized glass slide possessed approximately 95% transmittance in the wavelength range of 200 to 700 nm. The PDMS functionalized glass slides coated with lignin gel were found to have 85% transmittance. Moreover, the functionalized glass slide coated with silver nanocomposite doped lignin gel coating also had ~85% transmittance (Fig. 5c). The developed lignin nanocomposite gel coatings were also analyzed for their surface morphology through SEM analysis. It was observed that the incorporation of nanocomposites into the lignin gel coating emulsion did not change the morphology of the developed nanocomposite lignin gel-based coatings to a great extent when compared to the bare lignin gel coatings (Fig. 5d). Therefore, the nanocomposite lignin gel-based coatings can be utilized for further application in antimicrobial photodynamic therapy.

RB@AgLNCs doped lignin gel nanocoatings for antifungal and antibacterial photodynamic therapy

Due to the increasing number of hospital-acquired infections, patient safety and well-being are under increasing threat.[26] The major cause of a large number of such infections is the colonization of microbial biofilms on surfaces of medical devices such as catheters, endotracheal tubes, and prosthetics, which are implanted in millions of patients every year.[5] It has been found that fungal diseases are difficult to diagnose, which leads to high mortality rates in various parts of the world.[27,28] Moreover, antifungal drug resistance continues to limit the therapeutic options.[29,30]

Among the fungi, *Candida* species are the most prevalent biofilm pathogens and one of the leading causes of bloodstream infections in hospitals.[31] Therefore, there is an urgent need for the development of advanced strategies, such as coatings for targeting polymicrobial biofilms on medical devices.[32] Interestingly, lignin is known for its adhesive and antimicrobial properties which will be advantageous in coating formation.[33–35] The developed lignin-derived silver nanoformulations have been converted to nanocoatings by mixing with lignin solution and appropriate cross-linking agents to provide plasticizing properties through the formation of a nanocomposite gel (Fig. 6a). Fig. 6b illustrates the antimicrobial photodynamic effect of the developed lignin-based nanocoatings against *Candida tropicalis*. The exposure of *Candida tropicalis* to green LED did not show any significant reduction in fungal survival. The percentage of *Candida tropicalis* survival was observed to be reduced by ~7% in the instance of bare lignin coatings, the inhibition efficiency increases in the presence of green LED (~12% decrease in fungal survival). This is because the polyphenolic groups of lignin are associated with reactive oxygen species (ROS) generation in the presence of light, leading to increasing biological cytotoxicity. However, in the instance of lignin-based nanocoatings (with AgLNCs), the survival of *Candida tropicalis* colonies was 49.89% in the presence of green LED (3 W for 20 minutes). When the fungal colonies were treated with Lig_coat-RB@AgLNCs, the fungal growth was found to be around 42.6% (in the absence of LED), which was reduced to ~8.5% fungal growth (91.5% reduction in fungal survival) upon exposure to green LED for 20 minutes. This is due to the strong antimicrobial photodynamic effect of Rose Bengal (RB). The IC_{50} values of various samples against *Candida tropicalis* are summarized in Table 1. The developed bare lignin gel coatings along with lignin gel nanocoatings were also tested for their photodynamic antimicrobial efficacy against bacterial species. For this, *E. coli* (Gram-negative bacteria) was selected for further experimentation purposes (Fig. 6c). Interestingly, it was observed that the trend of antimicrobial activity of the developed probes was consistent with the bacterial species as with the fungal cells. However, the effect was slightly higher than *Candida tropicalis*, which is revealed by approximately 98% reduction in the bacterial growth upon treatment with Lig_coat-RB@AgLNCs in the presence of green LED (3 W for 20 minutes). This can be attributed to the eukaryotic nature of *Candida*

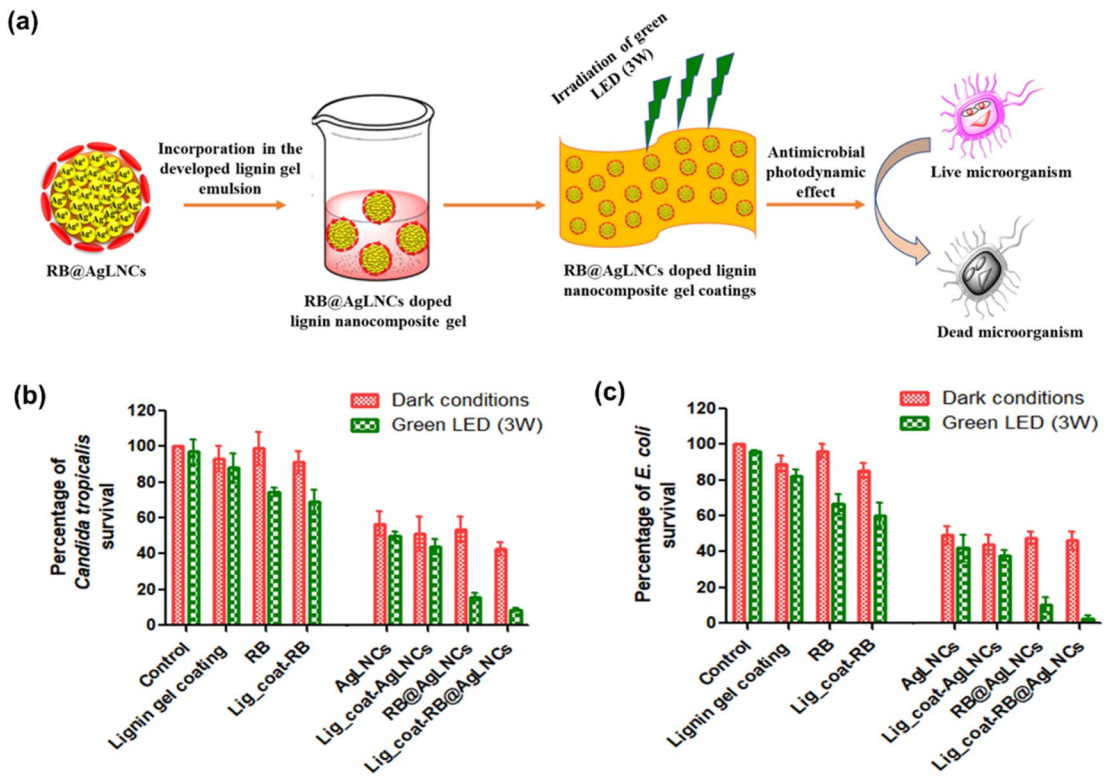

Fig. 6 (a) Schematic representation of the development of lignin gel and its utilization in antimicrobial photodynamic therapy; (b) antimicrobial photodynamic therapy of various agents against *Candida tropicalis*; (c) antimicrobial photodynamic therapy of various agents against *E. coli*.

Table 1 IC_{50} values of various samples against *Candida tropicalis* in the presence and absence of light

S. no.	Sample	No LED (μg mL^{-1})	With green LED (μg mL^{-1})	Fold decrease
1	Lignin gel coating	162.06 ± 0.91	136 ± 0.48	1.19
2	Rose Bengal	—	12.09 ± 0.26	—
3	AgLNCs	8.31 ± 0.98	5.81 ± 0.71	1.43
4	RB@AgLNCs	8.04 ± 0.81	5.48 ± 0.46	1.46
5	Lig-coat-RB@AgLNCs	15.64 ± 0.63	2.68 ± 0.59	5.83

tropicalis. The values for the antifungal efficacy of the various probes are summarized in Table S2 (ESI).†

The antimicrobial nanocoatings developed in this work have a great societal impact, in terms of coating various biomedical devices (surgical instruments, infected materials), masks, fabrics and common surfaces. Further, complete disinfection can be achieved through the application of an appropriate light source. Fig. 7a illustrates the disinfection of biomedical devices using the lignin gel-based nanocoatings. To further examine the effect of antimicrobial nanocoatings on different substrates, various surfaces (coated with lignin-based nanocomposite gels) were subjected to antimicrobial photodynamic therapy. Due to the majority of fungal infections reported in the literature being nosocomial, different lignin nanocomposite gels were coated over borosilicate glass surfaces and tested against fungal species only. All the coated as well as uncoated surfaces were transferred to freshly prepared growth media after incubation with *Candida tropicalis*, and allowed to grow for 18 h at 37 °C (Fig. 7b).

It was observed that the media became turbid for uncoated surfaces, revealing the presence of live fungal cells. However, in the case of the surfaces coated with RB@AgLNCS doped lignin gel, the media were clear and without any turbidity.

For further evaluation of the antifungal photodynamic efficacy of the developed nanocoatings, a 20 μL aliquot of fungal suspension (10^6 CFU per mL) in saline was placed on the lignin

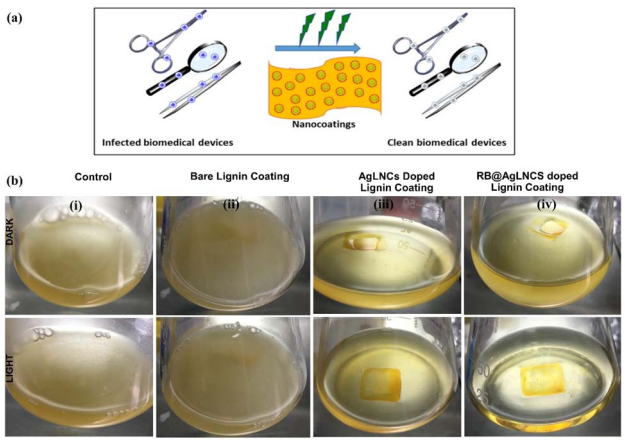

Fig. 7 (a) Schematic representation of disinfection of various biomedical devices using the developed lignin-based nanocoatings, (b) digital pictures of the different substrates: (i) control (ii) bare lignin coating, (iii) AgLNCs doped lignin nanocoating, and (iv) RB@AgLNCs doped lignin coating, incubated with a droplet of *Candida tropicalis* at 37 °C for 20 minutes in the dark and light (3 W green LED) and subsequently dipped in broth.

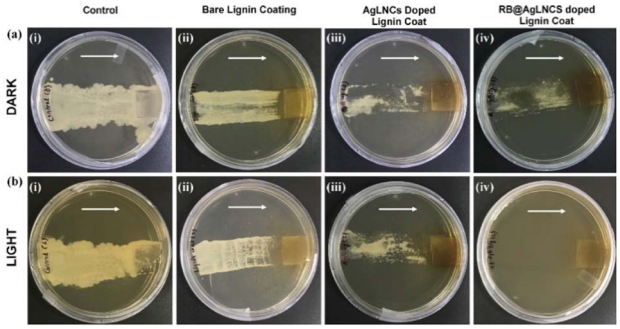

Fig. 8 Antifungal photodynamic therapy studies using dragging on agar plates. Digital pictures of various substrates: (i) control, (ii) bare lignin coating, (iii) AgLNCs doped lignin coating, and (iv) RB@AgLNCs doped lignin coating, incubated with a droplet of *Candida tropicalis* at 37 °C for 20 minutes under (a) dark conditions and (b) light (3 W green LED) and subsequently dragged on agar plates.

gel and nanocomposite gel coated surfaces followed by incubation for 20 minutes under light as well as dark conditions. The coated surfaces were then dragged on the agar plates to deduce their efficacy (Fig. 8). In the case of RB@AgLNCs doped lignin gel nanocoatings dragged over the agar plates, up to 95% reduction in fungal growth was observed. In contrast, thick fungal lawns were observed in the instance of uncoated surfaces displaying the exemplary antimicrobial efficacy of the coatings. The direction of dragging of coated surfaces on the agar plates is indicated by the arrows. Hence, the Lig-coat-RB@AgLNCs coating effectively reduces bacterial load after green LED exposure, thereby rendering it suitable to be employed on diverse biomedical equipment and implants. This observation also shows that the covalent coating composition was effective in killing microbes even after repeated examinations.

Experimental section

Synthesis of lignin gel

For the synthesis of the gel emulsion of lignin, alkali lignin (15 weight%) was dissolved in deionized water. This was followed by the addition of plasticizers, *i.e.* glycerol, glyoxal, and poly(-vinyl alcohol). 5% PVA and 2% glyoxal were found to be optimum for the development of lignin gel. The concentration of the plasticizers ranged from 1 to 5% to evaluate the optimum value. The solution was subjected to stirring conditions (200 rpm) for 15 minutes. After this, the reaction mixture was subjected to incubation at 60 °C for 30 minutes until a gel emulsion was developed.

Synthesis of Lignin-RB@AgLNCs nanocomposite gel

The synthesis of AgLNCs and RB@AgLNCs was carried out based on our previously published works.[3] For the development of the lignin-based nanocomposite gel, the pre-synthesized RB@AgLNCs (5% aqueous solution) were mixed with the precursor gel solution. This reaction mixture was then incubated at 60 °C for 30 minutes till it developed into a thick gel. For comparison, the AgLNCs-based nanocomposite gel was prepared in a similar manner. The lignin nanocomposite gel was then characterized and deposited onto a glass substrate to develop a coating.

Deposition of lignin bare gel coatings and nanocomposite coatings

Prior to use, the glass slides were immersed in ethanol and sonicated for 16 minutes, followed by drying at 120 °C. Firstly, a mixture of PDMS [poly(dimethyl siloxane)] (5 weight %) in hexane was prepared and applied to the glass slides to functionalize them. The slides were placed in an oven at 70 °C for 40 minutes to ensure the cross-linking initiation of PDMS. In order to fabricate the lignin-based coatings, the gel precursor solution was sprayed evenly using a spray bottle on the substrate surface, *i.e.* glass slide (1×2.5 inch^2). The glass slide was allowed to dry at 60 °C in an oven to develop a thin gel coating. Another simplified method used for the fabrication of lignin gel coatings was spreading the synthesized gel using a fine brush over the glass slide. This procedure was performed until the gel was evenly coated over the glass slide. The coatings were also developed using a customized dip coater, for which the glass slide was fixed on the slide holder, which was utilized to dip the glass slide into the gel emulsion kept below. For the appropriate development of lignin-based coatings, the number of cycles fixed for dip coating is 20. The wet time was kept at 20 minutes, followed by a drying time of 10 minutes.

Characterization of the lignin gel

Optical microscopy. For the surface analysis of the developed coatings over glass slides, they were observed under a bright field microscope. The optical transmittance of the glass slides coated with lignin coatings was studied with a UV-vis spectrophotometer in the range of 250 to 700 nm.

Rheology and FTIR analysis. To perform rheology studies, a pressure of 2 N was applied to the lignin gel using the planar probe head (having a diameter of 25 mm) of the rheometer. The viscosity of the samples was measured against an applied shear rate of up to 200 s^{-1}. For the FTIR analysis, the nanocoating samples were freeze-dried and measured with an ATR accessory (64 scans and resolution of 4 cm^{-1}).

Transmittance analysis. For the transmittance analysis, the coating samples (bare lignin as well as nanocoatings) were analyzed using a UV-vis spectrophotometer for their visible light transmittance. For this, the samples were coated on the surfaces of thoroughly cleaned glass slides, dried, and analyzed for transmittance in the range of 200–700 nm.

Elemental analysis. The total carbon, hydrogen, nitrogen, and sulfur (CHNS) contents of the newly developed lignin coatings and nanocoatings were determined using a CHNS analyzer. For this, the samples were freeze-dried, crushed, and weighed. This was followed by mixing of the samples with an oxidizer in a tin capsule, and combustion in a reactor at 1000 °C. A thermal conductivity detector (set at 290 °C) was then used for the final quantification.

Antimicrobial photodynamic therapy of the lignin gel nanocoatings

Colony counting method. For colony counting, *Candida tropicalis* was grown in MGYP (mannose, glucose, yeast extract and peptone) broth at 37 °C for approximately 12 h. Also, the bacterial strain (*E. coli*) was grown in Luria Bertani broth at 37 °C for 12–18 h. Both the strains were subjected to orbital shaking (150 rpm) in a 20 mL Erlenmeyer flask and allowed to grow until the OD_{600} value reached 0.6. The cells were then collected in a sterile microcentrifuge tube and washed with PBS. The pelleted cells were resuspended in PBS and incubated with all the samples at the concentration of 1 μg mL^{-1} in deionized water. Each set-up of lignin nanocoating treated fungal and bacterial cells was then individually illuminated with a green LED (3 W) for 15 min. The fungal cells were then plated, followed by the counting of colonies in each plate.

Visual turbidity analysis. *Candida tropicalis* was allowed to grow for 12 h in MGYP broth at 37 °C under constant shaking conditions. Then the fungal cells were diluted to prepare a suspension in PBS ($\sim 10^6$ CFU per mL). The final cell suspension (20 μL aliquot) was placed on a 1×1 cm^2 borosilicate glass surface coated with lignin nanocomposite gel. The surfaces were subjected to illumination under green LED for 15 minutes at 37 °C. For control, another set of coated and uncoated surfaces was kept in the dark under similar conditions. All the surfaces were subsequently placed into freshly prepared nutrient broth (20 mL) individually, followed by incubation for 18 h. After incubation, the flasks were visually analyzed for the presence of any turbidity, and images of the flasks were captured for comparison purposes.

Dragging on agar plates. *Candida tropicalis* cells were grown for 12 h in MGYP broth at 37 °C with constant shaking. Then dilution of the fungal cells was done to prepare $\sim 10^6$ CFU per mL suspension in PBS. After this, a 20 μL aliquot of this cell suspension was placed on a 1×1 cm^2 borosilicate glass surface coated with nanocomposite lignin coatings as well as bare lignin coatings. The coated as well as uncoated surfaces were illuminated under green LED for 15 minutes at 37 °C. For control, another set of coated and uncoated surfaces was kept in the dark under similar conditions. After this, all the surfaces were subjected to dragging along the diameter and subsequently placed on MGYP agar plates. These plates were then subjected to incubation for 18 h at 37 °C and digital imaging. All the experiments were carried out in triplicates.

Conclusions

In this work, we have demonstrated a highly effective and simple method to develop lignin-based sustainable antifungal and antibacterial nanocoatings. Fluorescence microscopy

revealed the highly networked and cross-linked structure of the coatings, which were also found to be highly water-resistant, transparent, and adhesive. The incorporation of RB@AgLNCs in the lignin coatings leads to a reduction of the IC_{50} value against *Candida tropicalis* by 50 fold (in the presence of green LED) as compared to the bare lignin coating, which is an exemplary finding of this work. This inhibition reduces to 10 fold in the absence of green LED. The antifungal and antimicrobial photodynamic activities of all the samples were confirmed by testing the coated coverslips by dragging them on agar plates as well as visual turbidity analysis. Hence, this study demonstrates the effectiveness of Lig-coat-RB@AgLNCs to effectively inactivate both bacteria as well as a lethal fungal infectious agent, *i.e.*, *C. tropicalis* species upon green LED exposure at a significant amount. The developed material has the potential to exhibit effectiveness when used on a range of biomedical equipment and implants since distinct implant-associated infections have a comparable microbial population. These findings led us to confirm the high applicability of the developed lignin-based sustainable nanocoatings for the disinfection of biomedical devices.

Data availability

The data supporting this article have been included as part of the ESI.†

Conflicts of interest

There are no conflicts to declare.

Acknowledgements

The authors would like to acknowledge the Department of Biotechnology (DBT), Govt. of India for funding and infrastructural support. JB thanks the Department of Science and Technology (DST), Govt. of India for funding under the Agrotech scheme. JB would also like to acknowledge DBT for providing funding under lignin valorization flagship project. SC would like to thank the Indian Council of Medical Research (ICMR) for the Senior Research Fellowship. KG would like to thank CIAB Mohali for the Junior Research Fellowship and SP would like to thank the Council of Scientific and Industrial Research (CSIR), India for the Senior Research Fellowship. The authors would also like to acknowledge CIAB Mohali for providing access to the instrumentation facilities.

References

1 W. Wang, X. N. Yang, Y. Wang, Y. Fan and J. N. Xu, *RSC Adv.*, 2021, **11**, 4365–4372.
2 F. H. Isikgor and C. R. Becer, *Polym. Chem.*, 2015, **6**(25), 4497–4559.
3 (*a*) S. Chandna, N. S. Thakur, R. Kaur and J. Bhaumik, *Biomacromolecules*, 2020, **21**, 3216–3230; (*b*) S. Chandna, N. S. Thakur, Y. N. Reddy, R. Kaur and J. Bhaumik, *ACS Biomater. Sci. Eng.*, 2019, **5**(7), 3212–3227.
4 (*a*) R. Sorey, A. Salaghi, P. Fatehi and T. H. Mekonnen, *RSC Sustainability*, 2024, **2**, 804–831; (*b*) S. Ghosh, R. Mukherjee, D. Basak and J. Haldar, *ACS Appl. Mater. Interfaces*, 2020, **12**, 27853–27865.
5 D. F. Guevara-bernal, M. Y. Cáceres Ortíz, J. A. Gutiérrez Cifuentes, J. Bastos-arrieta, C. Palet and A. M. Candela, *Water*, 2022, 1796.
6 A. Morales, J. Labidi and P. Gullón, *Sustainable Mater. Technol.*, 2022, **31**, e00369.
7 X. Liu, M. Li, X. Li, M. Ge, S. Liu, S. Li, J. Li, J. Ding, A. J. Ragauskas, W. Sun, T. D. James and Z. Chen, *Mater. Today Chem.*, 2022, **26**, 101000.
8 S. Chandna, S. Paul, R. Kaur, K. Gogde and J. Bhaumik, *ACS Appl. Polym. Mater.*, 2022, **4**, 8962–8976.
9 (*a*) D. D. S. Porto, B. M. Estevão, P. M. Pincela Lins, N. C. Rissi, V. Zucolotto and M. F. G. F. Da Silva, *ACS Appl. Polym. Mater.*, 2021, **3**, 5061–5072; (*b*) S. Chandna, M. C. A. Olivares, E. Baranovskii, G. Engelmann, A. Böker, C. C. Tzschucke and R. Haag, *Angew. Chem., Int. Ed.*, 2024, e202313945.
10 (*a*) N. Martins and C. F. Rodrigues, *J. Clin. Med.*, 2020, **9**, 722; (*b*) S. Paul, B. Yadav, M. D. Patil, A. K. Pujari, U. Singh, V. Rishi and J. Bhaumik, *Mater. Adv.*, 2024, **5**, 1903–1916.
11 (*a*) K. Gogde, S. Paul, A. K. Pujari, A. K. Yadav and J. Bhaumik, *J. Med. Chem.*, 2023, **66**, 13058–13071; (*b*) A. K. Pujari, R. Kaur, Y. N. Reddy, S. Paul, K. Gogde and J. Bhaumik, *J. Med. Chem.*, 2024, **67**(3), 2004–2018.
12 S. Paul, N. S. Thakur, S. Chandna, Y. N. Reddy and J. Bhaumik, *J. Mater. Chem. B*, 2021, **9**, 1592–1603.
13 A. Boarino, H. Wang, F. Olgiati, F. Artusio, M. Özkan, S. Bertella, N. Razza, V. Cagno, J. S. Luterbacher, H. A. Klok and F. Stellacci, *ACS Sustain. Chem. Eng.*, 2022, **10**, 14001–14010.
14 E. M. Kojic and R. O. Darouiche, *Clin. Microbiol. Rev.*, 2004, **17**, 255.
15 K. M. Sakita, P. C. V. Conrado, D. R. Faria, G. S. Arita, I. R. G. Capoci, F. A. V. Rodrigues-Vendramini, N. Pieralisi, G. B. Cesar, R. S. Gonçalves, W. Caetano, N. Hioka, E. S. Kioshima, T. I. E. Svidzinski and P. S. Bonfim-Mendonça, *Future Microbiol.*, 2019, **14**, 519–531.
16 F. B. Cavassin, J. L. Baú-Carneiro, R. R. Vilas-Boas and F. Queiroz-Telles, *Infect. Dis. Ther.*, 2021, **10**, 115–147.
17 J. John, A. Loo, S. Mazur and T. J. Walsh, *Expert Opin. Drug Metab. Toxicol.*, 2019, **15**, 881–895.
18 S. L. Iconaru, M. V. Predoi, P. Chapon, S. Gaiaschi, K. Rokosz, S. Raaen, M. Motelica-Heino and D. Predoi, *Coatings*, 2021, **11**, 464.
19 S. Demartis, A. Obinu, E. Gavini, P. Giunchedi and G. Rassu, *Dyes Pigm.*, 2021, **188**, 109236.
20 Y. N. Reddy, K. Gogde, S. Paul and J. Bhaumik, *Biomass for Bioenergy and Biomaterials*, 2021, pp. 31–64.
21 Y. N. Slavin, K. Ivanova, J. Hoyo, I. Perelshtein, G. Owen, A. Haegert, Y. Y. Lin, S. Lebihan, A. Gedanken, U. O. Häfeli, T. Tzanov and H. Bach, *ACS Appl. Mater. Interfaces*, 2021, **13**, 22098–22109.
22 S. Glass, T. Rüdiger, J. Griebel, B. Abel and A. Schulze, *RSC Adv.*, 2018, **8**, 41624–41632.

23 A. Beaucamp, M. Muddasar, I. S. Amiinu, M. Moraes Leite, M. Culebras, K. Latha, M. C. Gutiérrez, D. Rodriguez-Padron, F. del onte, T. Kennedy, K. M. Ryan, R. Luque, M. M. Titirici and M. N. Collins, *Green Chem.*, 2022, **24**, 8193–8226.
24 T. P. M. Ferreira, N. C. Nepomuceno, E. L. G. Medeiros, E. S. Medeiros, F. C. Sampaio, J. E. Oliveira, M. P. Oliveira, L. S. Galvão, E. O. Bulhões and A. S. F. Santos, *Prog. Org. Coat.*, 2009, **133**, 19–26.
25 S. Glass, T. Rüdiger, J. Griebel, B. Abel and A. Schulze, *RSC Adv.*, 2018, **8**, 41624.
26 B. R. Coad, H. J. Griesser, A. Y. Peleg and A. Traven, *PLoS Pathog.*, 2016, **12**, 1005598.
27 M. L. Rodrigues and J. D. Nosanchuk, *PLoS Neglected Trop. Dis.*, 2020, **14**, e0007964.
28 N. P. Wiederhold, *Infect. Drug Resist.*, 2017, **10**, 249–259.
29 J. Beardsley, C. L. Halliday, S. C. A. Chen and T. C. Sorrell, *Future Microbiol.*, 2018, **13**, 1175–1191.
30 M. L. Rodrigues and J. D. Nosanchuk, *PLoS Neglected Trop. Dis.*, 2020, **14**, e0007964.
31 G. Brunetti, A. S. Navazio, A. Giuliani, A. Giordano, E. M. Proli, G. Antonelli and G. Raponi, *PLoS One*, 2019, **14**, e0224678.
32 T. T. Yao, J. Wang, Y. F. Xue, W. J. Yu, Q. Gao, L. Ferreira, K. F. Ren and J. Ji, *J. Mater. Chem. B*, 2019, **7**, 5089–5095.
33 D. Stewart, *Ind. Crops Prod.*, 2008, **27**, 202–207.
34 M. Stanisz, Ł. Klapiszewski, M. N. Collins and T. Jesionowski, *Mater. Today Chem.*, 2022, **26**, 101198.
35 N. H. Abu Bakar, W. N. Wan Ismail, H. Mohd Yusop and N. F. Mohd Zulkifli, *New J. Chem.*, 2024, **48**, 933–950.